Frequency analysis of the dielectric constant of $YBa_2Cu_3O_7$ Josephson junctions fabricated on bicrystalline substrates

M. A. Navacerrada,[1] M. L. Lucía,[2,*] L. L. Sánchez-Soto,[3] F. Sánchez-Quesada,[2] E. Sarnelli,[4] and C. Nappi[4]
[1]*Departamento de Física e Instalaciones, Escuela Técnica Superior de Arquitectura, Universidad Politécnica, Avda. Juan de Herrera 4, 28040 Madrid, Spain*
[2]*Departamento de Física Aplicada III (Electricidad y Electrónica), Facultad de CC. Físicas, Universidad Complutense, Avda. Complutense s/n, 28040 Madrid, Spain*
[3]*Departamento de Óptica, Facultad de Ciencias Físicas, Universidad Complutense, Avda. Complutense s/n, 28040 Madrid, Spain*
[4]*Istituto di Cibernetica "E. Caianello" CNR, Via Campi Flegrei, 34 Pozzuoli, Italy*
(Received 2 February 2006; revised manuscript received 8 April 2006; published 12 July 2006)

We have studied the electromagnetic parameters of $YBa_2Cu_3O_7$ Josephson junctions fabricated on bicrystalline substrates with different angles tilted around the [100] and [001] axis. Changing a technological parameter such as the junction width permits change to the resonant frequency of the barrier cavity. This change in the resonance frequency allows one to determine a frequency dependent dispersion relation of the dielectric constant $\varepsilon(\omega)$. We have explored the proximity to a resonance in the dielectric response and analyzed its resonance frequency and damping constant. In terms of a *RLC* circuital equivalence additional information on the inductive response is presented as a comparative study of junctions fabricated on substrates with different bicrystalline misorientations.

DOI: 10.1103/PhysRevB.74.024507 PACS number(s): 74.50.+r

I. INTRODUCTION

The epitaxial growth of $YBa_2Cu_3O_7$ (YBCO) thin films on $SrTiO_3$ (STO) bicrystalline substrates has become a widely used technique for the fabrication of superconducting grain boundary Josephson junctions (GBJJs). The pioneering studies published in the literature on GBJJs were mainly based on the properties of [001] tilt bicrystalline substrates.[1] However, research on YBCO GBJJs fabricated on other bicrystal geometries are coming up in recent years. For instance, detailed comparative studies of [100] tilt boundary junctions fabricated on "valley" type bicrystalline substrates and conventional junctions fabricated on [001] tilt bicrystals have been presented by Poppe *et al.*[2,3] In these reports the [100] tilt boundary junctions show interesting properties for device applications: a high critical current × normal resistance product of the barrier (I_CR_N) and a low degree of faceting in comparison to [001] tilt boundaries. In this same line, it would be very interesting to investigate the properties of GBJJs fabricated on substrates tilted around both [100] and [001] axis.

We have previously reported comparative studies of [001] and [100] tilt GBJJs in terms of the electromagnetic parameters. The capacitive response reveals different barrier natures and transport properties in [001] tilted bicrystals than in junctions fabricated on [100] tilted bicrystals.[4,5] Going into the electromagnetic properties of GBJJs, several articles have been published in the literature focusing on the Swihart velocity ($\bar{c}$) and the ratio of the dielectric constant to the thickness of the barrier $\left(\frac{\varepsilon}{t}\right)$ of [001] tilt junctions.[6–8] The $\frac{\varepsilon}{t}$ ratio is derived indistinctly by considering the hysteresis in the current-voltage (*I-V*) curves or by measuring the voltage of Fiske steps $V_n=\frac{n\phi_0\bar{c}}{2W}$, where n is the resonance number, W the junction width, and ϕ_0 the magnetic flux quantum.[9] As it can be deduced from this expression, changing W we are actually modifying V_n, so the resonant frequency $f_n=\frac{V_n}{\phi_0}$ for each fixed n. In all cases reported, a single value of the average $\frac{\varepsilon}{t}$ ratio is given for all the junctions independently of W. This average value is calculated by plotting the Fiske step voltage against the inverse of W and fitting the data to the relation $V_n=\frac{n\phi_0\bar{c}}{2W}$. Once $\bar{c}$ is deduced from the fitting, the $\frac{\varepsilon}{t}$ ratio is calculated by using the expression

$$\bar{c}=\left[c_0\left(\frac{t}{\varepsilon d}\right)^{1/2}\right], \tag{1}$$

where c_0 is the vacuum light velocity and d the effective magnetic junction length. The dependence of $\bar{c}$ on f_n is reported in some articles, but establishing no relation with a possible frequency dependence of $\frac{\varepsilon}{t}$.[6]

We propose to calculate a $\frac{\varepsilon}{t}$ ratio for each W, so for each f_n. This way we can establish a dispersion relation $\varepsilon(f_n)$, which is essentially the relation of ε with frequency (ω). This analysis has already been performed in a semiquantitative approach for [001] tilt junctions using 24° symmetric bicrystals: we showed the inadequacy of modeling the barrier as a perfect dielectric medium.[10] A *RLC* model was then presented which included the contribution of the kinetic inductance (L) associated to the superconducting filaments in the barrier. The aim of the present work is to explore in detail the curve $\varepsilon(f_n)$, so $\varepsilon(\omega)$. We are also extending the analysis to other bicrystal geometries ([001] tilt, [100] tilt, and [100] tilt-tilt) which are known to have different barrier structures and transport properties. We will show that in terms of the dielectric response of the barrier, a resonant behavior is always detected.

II. EXPERIMENTAL PROCEDURE

Grain boundary Josephson junctions based on YBCO were fabricated using bicrystalline substrates of STO with different symmetrical and asymmetrical tilt angles around

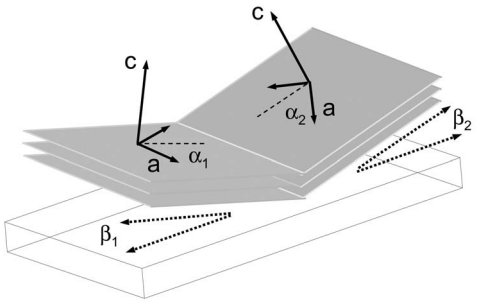

FIG. 1. Schematic representation of the [001] and [100] bicrystal orientations. The [001] axis of the electrodes are tilted in plane by angles α_1 and α_2. The case $\alpha_1=\alpha_2=0$ corresponds to a [100] tilt boundary. The left (right) [001] axis is tilted by an angle β_1 (β_2). The case $\beta_1=\beta_2=0$ corresponds to a [001] tilt boundary.

the [100] and [001] axis. A usual scheme to illustrate the different tilt bicrystalline substrates is shown in Fig. 1. The misorientation angles for the five geometrical configurations we have analyzed are indicated in Table I. In this report [100] tilt and [100] tilt-tilt bicrystal geometries are of the valley type where the [001] axis is tilted towards the grain boundary. YBCO films were epitaxially grown in a high pressure (3.4 mbar) pure oxygen dc sputtering system. In the deposition process the substrate temperature was 900 °C. The high quality of the YBCO thin films deposited on the bicrystalline substrates using this technique has been demonstrated in previous articles.[4,10,11] Films were patterned obtaining junction widths ranging between 2 and 20 μm for all the STO bicrystals. Electrical characterization has been carried out in a highly shielded cryostat and the external magnetic field was applied perpendicular to the substrate surface. The *I-V* curves for different values of the applied magnetic field have been measured using low-noise electronics. We have observed Fiske steps in all our samples. No doubts arose in their identification since the dependence of their intensity on the magnetic field is as predicted by the theory.[12] In the analysis of the dielectric response of the barrier, $\bar{c}$ has been determined by the position of the Fiske step $n=1$ (V_1) and $\frac{\varepsilon}{t}$ ratios are calculated using expression (1). Since the thickness δ of our films is always smaller than the London penetration depth (λ_L), d has to be calculated using the expression $\lambda=\lambda_L \coth\left(\frac{\delta}{\lambda_L}\right)$.[12] The whole procedure is repeated for each substrate geometry and for each W.

TABLE I. Values of the bicrystal α and β misorientation angles for all our GBJJs.

Bicrystal Geometry		α_1	α_2	β_1	β_2
[001] tilt	12° [001] asymmetric	0	12°	0	0
	24° [001] symmetric	12°	12°	0	0
	24° [001] asymmetric	0	24°	0	0
[100] tilt	45° [100] asymmetric	0	0	0	45°
[100] tilt tilt	24° [001] symmetric	12°	12°	0	45°
	+45° [100] asymmetric				

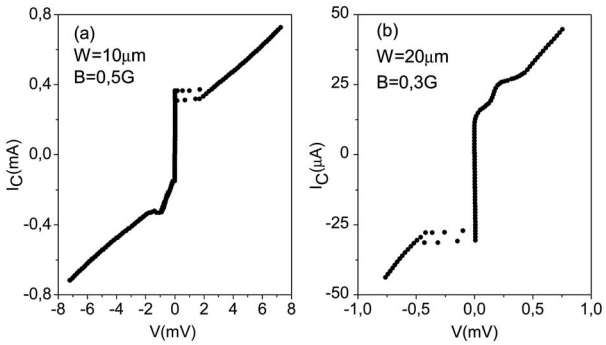

FIG. 2. *I-V* curves corresponding to: (a) 45° [100] tilt asymmetric and (b) 24° [001] tilt symmetric +45° [100] tilt asymmetric YBCO GBJJs for a fixed value of the magnetic field indicated in the plot. In both cases the *I-V* characteristics show hysteresis in one part of the curve. The hysteresis is large enough to extract the I_C and I_R values in order to calculate β_C.

III. RESULTS AND DISCUSSION

For the following discussion, particular care has been taken in order to eliminate possible sources of error. In this line, it is compulsory to ensure that the capacitances we are operating with are associated only to the grain boundary, with no confusing contributions from the STO bicrystalline substrate. The influence of the substrate on the dielectric behavior of the barrier has been reported in the literature.[7,8] In order to discard such contribution we have checked that in our working regime a linear relationship between the McCumber parameter (β_C) and the critical current (I_C) is fulfilled. Specifically, the predicted relationship for both parameters is $\beta_C=\frac{2eI_CR_N^2C}{\hbar}$ where e is the electronic charge, $\hbar$ is the Planck constant divided by 2π, R_N is the normal resistance of the junction, and C its capacitance.[13] For a fixed W, so for each particular junction, C is constant if no substrate contribution dominates, then a linear relation between β_C and I_C must be measured experimentally. The values of β_C and I_C can be experimentally varied changing the value of the magnetic field applied to the barrier. Moreover, the application of the magnetic field has the effect of modifying the frequency of the Josephson oscillations[7] and the dielectric response of the STO substrate is also frequency dependent. In fact at low frequencies the relative dielectric constant can be large (below 200 GHz at 4.2 K).[14] If such a frequency range is reached the substrate may affect the capacitance determination of the barrier so that the linear relation between β_C and I_C would no longer be fulfilled.

β_C values have been obtained with Zappe's approximation[15] $\beta_C=\frac{[2-(\pi-2)\alpha]}{\alpha^2}$ in terms of the ratio $\alpha=\frac{I_R}{I_C}$ of the return current I_R to I_C. The values of I_R and I_C have been extracted from the *I-V* characteristics. Some examples of *I-V* curves are shown in Fig. 2. As an example, the plot of β_C versus I_C corresponding to the sample of Fig. 2 [curve (a)] is shown in Fig. 3. The relation between both magnitudes is approximately linear so we conclude that the substrate makes no appreciable contribution to the C value. In fact, at low temperatures Ransley *et al.*[7] have shown that the substrate contributes to the capacitance at return voltages below

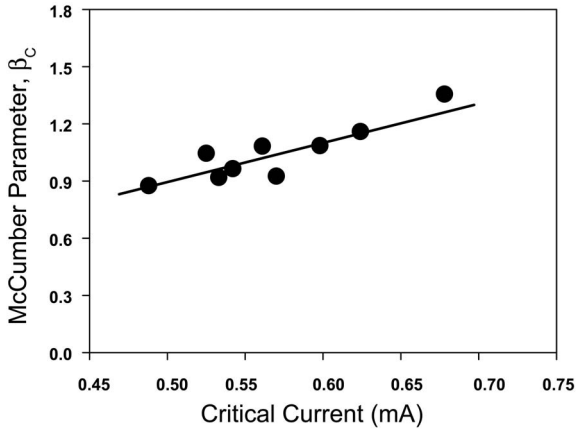

FIG. 3. Plot of the McCumber parameter (β_C) versus critical current for a junction with $W=10$ μm fabricated on a 45° [100] tilt asymmetric bicrytalline substrate. The straight line serves as a guide to the eye.

0.25 mV. The examples of Fig. 2 show that this limit is exceeded.

We have observed Fiske steps in our samples, supporting the idea of the junctions as resonators for the geometries studied where the barrier forms the effective dielectric medium. Some examples of Fiske steps evidence in the *I-V* curves are shown in Fig. 4. We have plotted the characteristics corresponding to four different bicrystal geometries. For the [100] tilt GBJJs with $\alpha_1=\alpha_2=\beta_1=0$ and $\beta_2=45°$ the presence of Fiske steps was already shown in Fig. 2. The V_I position of the Fiske step is estimated as the voltage corresponding to the maximum current in the step. The presence of flux-flow resonances and excess current in some cases makes it difficult to determine the Fiske step position after subtracting the term V/R_N to the experimental *I-V* curves. It is important to point out at this stage that the position of the first Fiske step V_1 is always over the approximated limit of 0.3 mV fixed by Ransley *et al.*[7] These authors claim that over this voltage limit, the frequency is large enough so that the dielectric contribution of the substrate is low. Following their procedure, we conclude that our data deduced from the position of these resonances are only related to the grain boundary.

We have observed for all our junctions that the $\frac{\varepsilon}{t}$ ratio increases when f_1 of the resonant barrier cavity increases. This result gives us the clue to consider a proximity to a resonance in the dielectric response. Actually, by changing W in our GBJJs we are sweeping in frequency since $\omega=f_1(W)$. Considering this possibility, we have explored two equivalent approaches. On the one hand, and from a circuital point of view, an inductive term is added to reach a *RLC* analogy where R accounts for the transport of quasiparticles and C for the dielectric response of the barrier. Because of the large magnetic penetration depth of YBCO, the kinetic inductance L must be taken into account in the model. On the other hand, and from a physical point of view, the description of the resonator in YBCO GBJJs as a perfect dielectric cavity is no longer valid and the contribution of electrical losses must be taken into account. In this sense, it is possible to explore the well-known dispersion relation[16] $\varepsilon(\omega)$

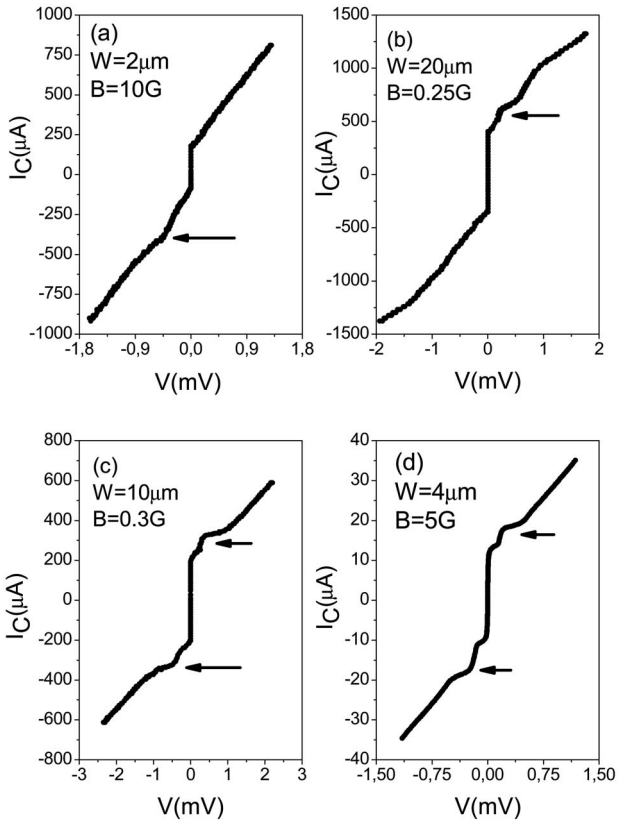

FIG. 4. *I-V* curves corresponding to four bicrystal geometries: (a) 12° [001] tilt asymmetric, (b) 24° [001] tilt symmetric, (c) 24° [001] tilt asymmetric, and (d) 24° [001] tilt symmetric +45° [100] tilt asymmetric. The junction width and the magnetic field are indicated in the plot. In all the *I-V* characteristics the Fiske step $n=1$ (indicated by the arrows) is observed at least in one part (positive or negative) of the curve.

$$\varepsilon = \varepsilon_0 + \frac{NQ^2}{m}\frac{\omega_0^2 - \omega^2}{(\omega_0^2 - \omega^2)^2 + 4\gamma^2\omega^2}, \tag{2}$$

where ε_0 is the vacuum dielectric constant, N the number of atoms per volume unit, Q the charge carrier per unit cell, m the mass of free electrons, and γ the damping constant. We have fitted our data to expression (2) considering $t\approx 3$ nm in order to deduce ε from the experimental $\frac{\varepsilon}{t}$ ratios.[17] In the fit $\frac{NQ^2}{m}$, ω_0 and γ have been considered as free parameters. For all the junctions the $\frac{NQ^2}{m}$ ratio is in the range of 10^{22} so the carrier density is about 10^{21} cm^{-3} which is consistent with the values reported in the literature for YBCO GBJJs.[18] A detailed analysis of the fits and the value of n for each geometry will be published later.

In Table II we have quoted the values obtained for ω_0 and γ for substrates with the different bicrystalline misorientations. We can observe that ω_0 decreases with the misorientation angle while γ increases. The behavior of these two parameters with the bicrystal geometry can give us some insight about the properties of the barrier. From the well known expression of the resonance frequency in an *RLC* circuit, $\omega_0=\frac{1}{\sqrt{LC}}$, it is possible to calculate L. Results are

TABLE II. Resonance frequency (ω_0) and damping constant (γ) obtained for all the bicrystal geometries. The kinetic inductance (L) is quoted only for junctions with $W=10$ μm.

Bicrystal Geometry	ω_0 ($\times 10^{11}$ Hz)	γ ($\times 10^{10}$ Hz)	L ($W=10$ μm) ($\times 10^{-11}$ H)
12° [001] asymmetric	7.41	1.80	4.43
24° [001] symmetric	4.47	2.50	7.54
24° [001] asymmetric	4.24	2.23	8.20
45° [100] asymmetric	3.30	3.26	10.25
24° [001] symmetric +45° [100] asymmetric	2.90	3.53	14.03

shown also in Table II, where for the sake of clarity only the GBJJs with $W=10$ μm are presented; for other widths the tendency is the same. In any case, for all the widths, L increases with the misorientation angle. Since the filamentary model describes the barrier shorted by parallel superconducting paths, an increase of L implies a decrease of the number of filaments, then a more insulating or semiconducting nature of the barrier. Atomic force microscopy images of YBCO thin films deposited on [100] valley tilted bicrystals reveal a low surface roughness. However, when the [100] tilt boundary is of the "roof" type, so when the [001] axis is tilted away from the grain boundary, a much wider and deeper surface suppression has been observed.[2] Since the electromagnetic parameters are related to the microscopic nature of the grain boundary, different results may be obtained with [100] tilted bicrystals of the roof type.

We also know that changing from 24° [001] symmetric to 45° [100] asymmetric GBJJs the modeling of the barrier may change from a filamentary description to a tunnel transport context.[4,5,19,20] This tendency is also confirmed in this analysis: as shown in Table II in terms of γ, when the misorientation angle increases the number of filaments decreases and the normal resistance of the barrier increases, so higher is the damping of the resonant system.

IV. CONCLUSIONS

In summary we have shown that the barrier of all our GBJJs can be modeled as a dielectric medium with losses. Our data $\varepsilon(f_1)$ can be fitted to the expression $\varepsilon(\omega)$ that describes the behavior of ε close to a resonance in a dielectric medium. In terms of the circuital equivalence *RLC*, we can also obtain some additional information on the inductive response of the barrier. The values reported for ω_0 and γ show a tendency to a more semiconductive behavior with the increase of the misorientation angle. This is in accordance with electrical characterizations previously performed on [001] tilt ($\alpha_1=\alpha_2=12°$) and [100] tilt ($\beta_1=0$, $\beta_2=45°$) GBJJs. In this sense, the consistency of a frequency dependence of the dielectric constant in YBCO GBJJs can bring new insight for recent bicrystalline geometries such as [100] tilt-tilt.

ACKNOWLEDGMENTS

This work was supported by the CICYT Grant No. BMF2001-1419, the ESF Network "Phi-shift," the project DG236RIC "NDA" and the TRN "DeQUACS."

*Corresponding author. E-mail address: mllucia@fis.ucm.es

[1] D. Dimos, P. Chaudhari, and J. Mannhart, Phys. Rev. B **41**, 4038 (1990).
[2] U. Poppe, Y. Y. Divin, M. I. Faley, J. S. Wu, C. L. Jia, P. M. Shadrin, and K. Urban, IEEE Trans. Appl. Supercond. **11**, 3768 (2001).
[3] Y. Y. Divin, U. Poppe, C. L. Jia, P. M. Shadrin, and K. Urban, Physica C **372–376**, 115 (2002).
[4] M. A. Navacerrada, M. L. Lucía, L. L. Sánchez-Soto, F. Sánchez Quesada, E. Sarnelli, and G. Testa, Phys. Rev. B **71**, 014501 (2005).
[5] M. A. Navacerrada, M. L. Lucía, L. L. Sánchez-Soto, F. Sánchez-Quesada, E. Sarnelli, and G. Testa, IEEE Trans. Appl. Supercond. **15**, 169 (2005).
[6] D. Winkler, Y. M. Zhang, P. A. Nilsson, E. A. Stepantsov, and T. Claeson, Phys. Rev. Lett. **72**, 1260 (1994).
[7] J. H. T. Ransley, P. F. McBrien, G. Burnell, E. J. Tarte, J. E. Evetts, R. R. Schulz, C. W. Schneider, A. Schmehl, H. Bielefeldt, H. Hilgenkamp, and J. Mannhart, Phys. Rev. B **70**, 104502 (2004).
[8] E. J. Tarte, P. F. McBrien, J. H. T. Ransley, R. H. Hadfield, E. I. Inglessi, W. E. Booji, G. Burnell, and J. E. Evetts, IEEE Trans. Appl. Supercond. **11**, 418 (2001).
[9] M. D. Fiske, Rev. Mod. Phys. **36**, 221 (1964).
[10] M. A. Navacerrada, M. L. Lucía, and F. Sánchez-Quesada, Phys. Rev. B **61**, 6422 (2000).
[11] M. A. Navacerrada, M. L. Lucía, and F. Sánchez-Quesada, Europhys. Lett. **54**, 387 (2001).
[12] A. Barone and G. Paterno, *Physics and Applications of the Josephson Effect* (Wiley, New York, 1982).
[13] D. E. McCumber, J. Appl. Phys. **39**, 3133 (1968).
[14] R. C. Neville, B. Hoeneisen, and C. A. Mead, J. Appl. Phys. **43**, 2124 (1972).
[15] H. Zappe, J. Appl. Phys. **44**, 137 (1972).
[16] H. Frohlich, *Theory of Dielectrics* (Oxford University Press, New York, 1968).
[17] J. W. Seo, B. Kabius, U. Dähne, A. Scholen, and K. Urban, Physica C **245**, 25 (1995).
[18] H. Hilgenkamp and J. Mannhart, IEEE Trans. Appl. Supercond. **9**, 3405 (1999).
[19] E. Sarnelli, G. Testa, D. Crimaldi, A. Monaco, and M. A. Navacerrada, Supercond. Sci. Technol. **18**, L35–39 (2005).
[20] E. Sarnelli, G. Testa, D. Grimaldi, A. Monaco, M. Adamo, and M. A. Navacerrada, IEEE Trans. Appl. Supercond. **15**, 245 (2005).